Journal of New Technology and Materials (JNTM)
J. New Technol. Mater.
Vol. 11, N°02 (2021)10-16

OEB Univ. Publish. Co.

Effect of incorporation of chromium on electronic, optical and magnetic properties of $KTaO_3$

K. Bettir[a], A. Bekhti Siad[b,*], M. Baira[a], C. Zouaneb[a] and R. Khenata[a]

[a]*Laboratory of Quantum Physics of Matter and Mathematical Modeling (LPQ3M), Mustapha Stambouli University of Mascara, Algeria*
[b]*Laboratory of Materials Applications and Environment (LMAE), Mustapha Stambouli University of Mascara, Algeria*

*Corresponding author, email: amarasiadmail@gmail.com

Selected paper of JMSM-2020, received date: Aug. 02, 2021 ; accepted date: Sep. 30, 2021

Abstract

In this study, the structural, electronic, optical and magnetic properties of undoped and Cr^{3+} doped KTaO3 compounds are investigated using the full potential linearized augmented plane wave method. The exchange-correlation potential is treated with the generalized gradient approximation (GGA) and modified Becke-Johnson potential (TB-mBJ) to improve the electronic structure calculations. These two compound are found to be semiconductors with indirect band gaps. The optical transitions are investigated via dielectric function along with other related optical constants such as refractive index and absorption coefficient. $KTaO_3$ compound display nonmagnetic behavior, whereas $KTaO_3$ doped Chromium show a ferromagnetic ground state. The magnetic properties in this theoretical study is also helpful for designing transition metal such as Chromium doped perovskite materials like KTaO3 compound for spin electonics performance.

Keywords: Perovskite materials; Semiconductor; optical properties ; magnetic properties; TB-mBJ

1. Introduction

Due to the increased demand for energy, it is possible to run out of non-renewable energy and the impact of these polluting energies on the environment by searching for alternative source of energy. Over the past several decades, many photocatalysts reportedly exhibited high photocatalytic activities for splitting water into a stoichiometric mixture of H2 and O2. 110Where, there is a lot of research on the sources of energy. The perovskite type (ABO_3) materials have received much attention due to their interesting superconductivity, catalytic characteristics, oxygen cathode reduction, and the electro- magnetic properties [1-3]. Beside, $KTaO_3$ is a good candidate for the study of the photocatalysts properties especially by doping atoms, for this reason this material is consider as a good host material for developing visible light photocatalysts [4]. In addition, $KTaO_3$ is one of these perovskite materials that is used in many applications such as red luminescence [5] and production of H2 with water splitting [6, 7]. The band gap energy of $KTaO_3$ is reported between 3.40 eV and 3.60 eV, which exhibits wide band gap semiconductor properties [8]. This means that the energy corresponds to ultraviolet region in the electromagnetic spectrum. Therefore, the aim of this work is to study the effect of doping atoms Cr^{+3} on $KTaO_3$ compound with an oxygen vacancy. Structural, electronic, magnetic and optic properties of pure and Cr^{+3} doped $KTaO_3$ compounds have been studied using the full linear augmented plane wave method (FP-LAPW) [9] within the density functional theory (DFT) [10].

2. Computational method

The electronic band structures were calculated by means of full-potential linearized augmented plane wave (FP-LAPW) method based on first principles density functional theory (DFT) as implemented in WIEN2k code [11]. This method is one of the most useful and reliable techniques for obtaining the ground state properties of materials based on DFT [12, 13]. Since calculations using the standard local-density (LDA) or Generalized Gradient Approximation (GGA) schemes for the exchange-correlation potential underestimate the band gaps of semiconductors, we have used the modified GGA known as Tran-Blaha modified Becke-Johnson (TB-mBJ) potential [14, 15]. The wave functions of the charge density and the potential in the interstitial region are expanded up to l_{max} = 10, as well as the energy cut-off of $R_{MT}.K_{max}$= 7.0 were kept fixed in our calculation, where R_{MT} denotes the smallest atomic sphere radius and K_{max} gives the magnitude of largest k-vector in the plane wave expansion. k-grid of 8x8x8_ was used for both pure $KTaO_3$ and $KTaO_3$ doped Chromium compounds. The tolerance of the total energy in self-consistency is less than 10^{-4}mRy per formula unit.

3. Results and discussion

3. 1 *Structural and electronic properties*

The ground state structural properties of $KTaO_3$ compound are studied using the Birch- Murnaghan equation of state [16]. This material adopts a cubic structure with space group Pm-3m (No.221). From the ground state volumes, as shown Fig. 1 and 2 the equilibrium lattice constants and ground state energies are evaluated. We can see that the curvature of total energy of the ferromagnetic (FM) state is more pronounced than the total energy of antiferromagnetic (AFM) state which gives a positive value of the total energy difference: $\Delta E = E_{AF} - E_{FM}$, so $Pb_2FeTaPO_6$ is stable in the FM phase. In Table 1, we report the calculated lattice parameters, which show good agreement with other experimental and theoretical works [17, 18, 19]. The doped $KTaO_3$ compound is formed by construction of a 2×2×2 supercell form of 40 atoms in order to replace Ta atoms with Cr atom. The principal charge of $KTaO_3$ compound is equal to zero, because, ion charge of K, Ta and O atoms are (+1), (+5) and (-2) respectively. When, Cr^{3+} atoms have been doped, one oxygen vacancy is formed to provide charge balance. This vacancy is the reason of formation of a defective structure and the neutrality of the compound is assured. Moreover, the calculated lattice parameter, bulk modulus and pressure derivative of bulk modulus were shown in Table1 and 2

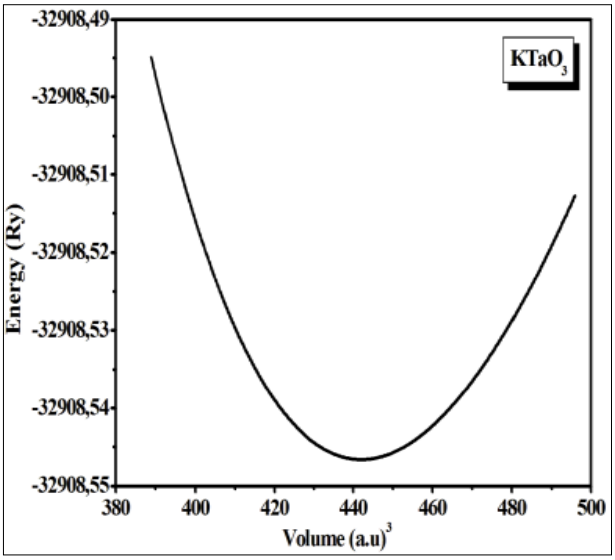

Figure 1. Optimization plots of the unit cell volume of $KTaO_3$

For a better understanding of the electronic structure of pure and doped $KTaO_3$, the dispersion curves of the electronic band structures along with high symmetry directions in the brillouin zone are investigated with mBJ-GGA as shown in Fig.3. From this figure, it is clear that perovskite $KTaO_3$ is a semiconductor with an indirect band gap Γ-M, with a value of 3.59eV, which is in agreement with the experimental one (3.75eV)[20].

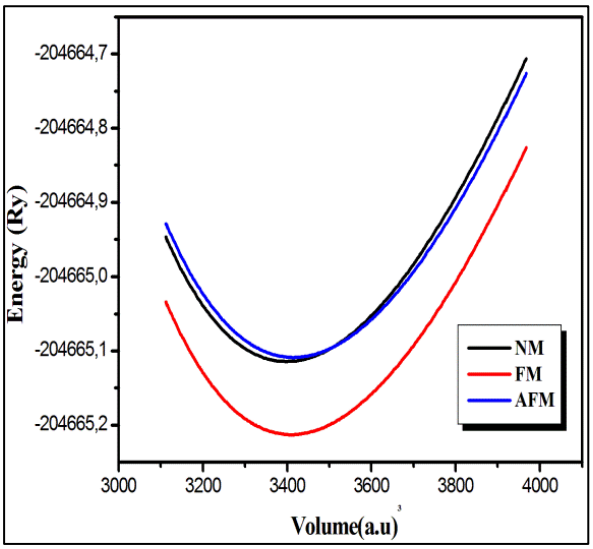

Figure 2. Optimization plots of the unit cell volume Cr doped $KTaO_3$.

Table 1: lattice parameter a (Å), bulk modulus B_0 (GPa) and its pressure derivatives B' $KTaO_3$, compared with the experimental data and other theoretical works.

	Present Work	Experiment	Other Calculations
a_0(Å)	4.0326	3.988[18]	3.950 [17]
B_0(GPa)	186,776	218[19]	224.850 [17]
B'	4,558		3.695 [17]

Table 2: Calculated lattice parameter a (Å), bulk modulus B_0 (GPa) and its pressure derivatives B 'of Cr doped $KTaO_3$

Compound	a_0(Å)	B_0(GPa)	B'
Cr doped $KTaO_3$	4.031	163.809	4.699

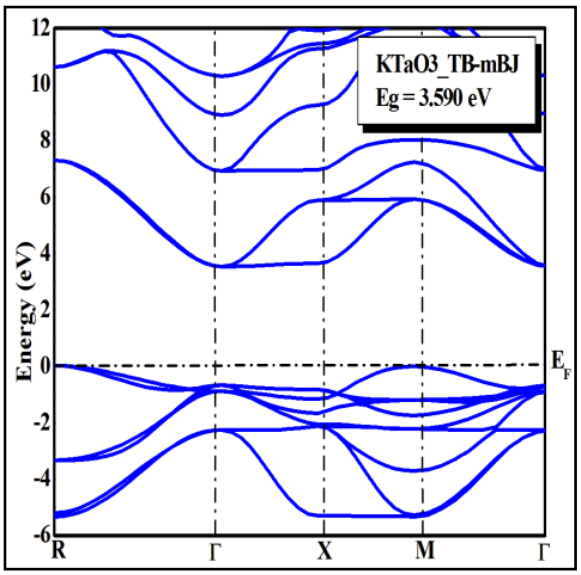

Figure 3. Electronic band structures of $KTaO_3$ are calculated by using TB-mBJ.

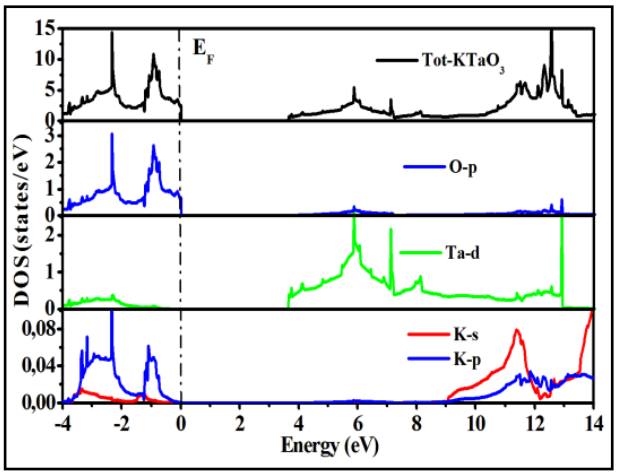

Figure 4. The total and partial density of states calculated for $KTaO_3$ by using TB-mBJ.

The study of the total density of states (TDOS) and partial density of states (PDOS) are in energy field from -4eV to 14eV as exhibited in Fig.4. The valence band lies between -4eV and Fermi level where we have an hybridization between the O 2p-states and Ta 5d-states. On the other side, in the conduction band the highest contribution is due to the 5d-states of Ta atoms of $KTaO_3$ compound.

The spin-polarized electronic bands structures studied of the doped $KTaO_3$ with Chromium are shown in Fig.5. Therefore, we can see from the figures that doped $KTaO_3$ are semi conductor for both spin states. In spin up state, it is found a direct band gap Γ- Γ and its value is 2.05eV, but we have an indirect band gap Γ-X of spin down state with a value of 2.40eV. This mean that bands gap values of the doped $KTaO_3$ agree with the visible region. Subsequently, we can study optoelectronic applications of this compound.

The calculated total density of states (TDOS) and partial density of states (PDOS) for Cr doped $KTaO_3$ are given Fig.6. In the total density of states, the valence band (VB) lies from -4eV to -0.6eV and the conduction band (CB) lies from 2eV to 6 eV for the spin up case. On the other hand, the valence band (VB) continues from -4eV until Fermi level and the conduction band (CB) continues from 2.5 eV to to 6 eV of the spin down case. In partial density of states (PDOS), we can clearly see that the 3d-states of Cr have a considerable impact on the electronic formation of perovskite $KTaO_3$.

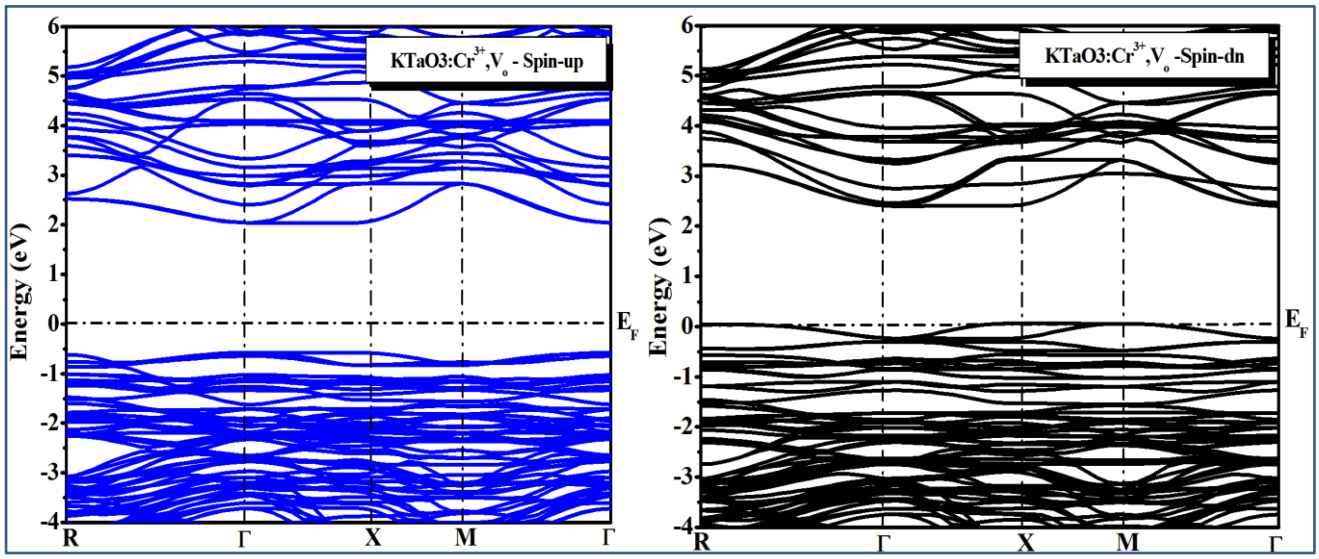

Figure 5. Spin-polarized electronic band structures of Cr doped $KTaO_3$ by using TB-mBJ.

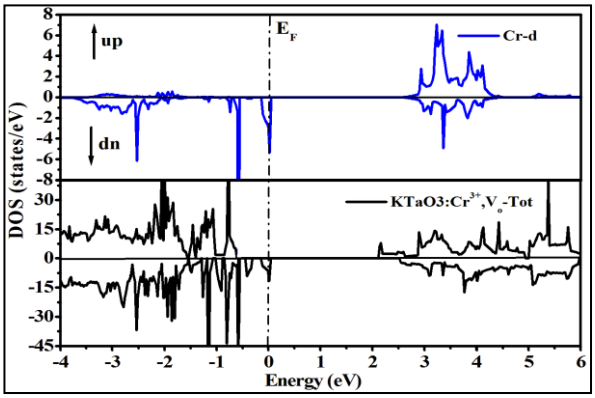

Figure 6. Spin-polarized total and partial density of Cr doped $KTaO_3$ by using TB-mBJ.

3. 2 Optical properties of $KTaO_3$ and $KTaO_3$:Cr^{3+},Vo

The optical materials have gained importance due to their wide application in lasers, optical communication windows, lenses, optical coatings, solar collectors and reflectors. The interaction of light with the valence electrons of materials is responsible for optical properties. The photon absorption with the electronic transition from the valence band to unoccupied conduction band especially at high symmetry points in the Brillouin zone, occurs in insulators and semiconductors.

The dielectric function $\varepsilon(\omega) = \varepsilon_1(\omega) + i\varepsilon_2(\omega)$ is well known to describe the optical response of the medium at

all photon energies. The imaginary part $\varepsilon_2(\omega)$ is directly related to the electronic band structure of a material and describes the absorptive behavior. The imaginary part of the dielectric function $\varepsilon_2(\omega)$ is given [21] by:

$$\varepsilon_2(\omega)=\frac{Ve^2}{2\pi\hbar m^2\omega^2}\int d^3k\sum_{nn'}\left|\langle kn|p|kn'\rangle\right|^2 \mathrm{f}(kn)\times[1-\mathrm{f}(kn')]\,\delta\left(\mathrm{E}_{kn}-\mathrm{E}_{kn'}-\hbar\omega\right) \quad (1)$$

where $\hbar\omega$ is the energy of the incident phonon, p is the momentum operator $\frac{\hbar}{i}\frac{\partial}{\partial x}$, $|\mathrm{kn}\rangle$ is the eigen function with eigenvalue E_{kn} and $f(\mathrm{kn})$ is the Fermi distribution function.

The real part $\varepsilon_1(\omega)$ of the dielectric function is given from the imaginary part using the Kramers-Kronig relation in the form [22]:

$$\varepsilon_1(\omega)=1+\frac{2}{\pi}P\int_0^{\infty}\frac{\omega'\varepsilon_2(\omega')}{\omega'^2-\omega^2}d\omega' \quad (2)$$

Where P implies the principal value of the integral.The FP-LAPW is a good theoretical tool for optical properties calculations. These properties give useful information about the internal structure of both $KTaO_3$ and $KTaO_3:Cr^{3+}$, V_o compounds. We use the mBJ-GGA method to calculate the optical properties of these compounds.

Following the theory presented in the second part of this paper, we have calculated the real ε_1 and imaginary ε_2 part of the dielectric function as function of the energy in the range of 0–55 eV, the results are presented in Fig. 7. Our calculations for ε_2 (ω) give 5.000, 6.120, 7.100, 10.500, 12.145, 13.112, 14.690, 17.436, 17.698, and 18.325 eV peaks between 5.000 and 18.4 eV, which should be compared with the experimental peaks around 18 eV [23]. The calculated static dielectric constant at zero energy is 3.76 for undoped $KTaO_3$.

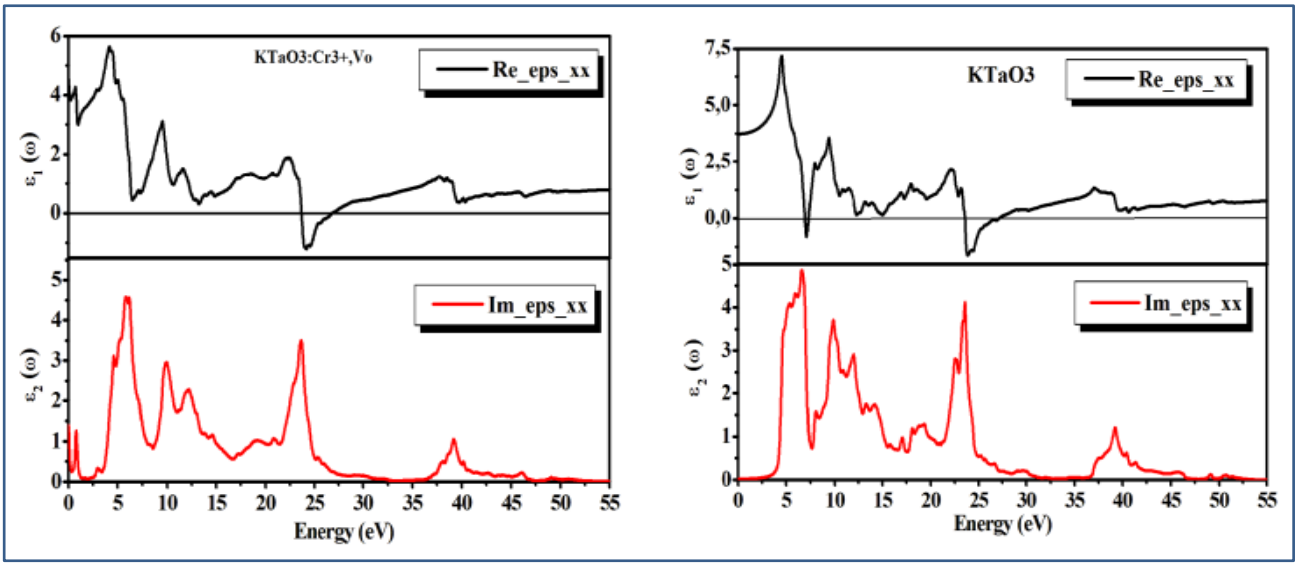

Figure 7. The calculated real and imaginary parts of dielectric function for doped and undoped $KTaO_3$compound ε_1 real part and ε_2 imaginary part.

The real and imaginary part of the dielectric function of the doped and defective $KTaO_3$ compounds is shown in Fig. 7. The static dielectric constants for $KTaO_3:Cr^{3+},V_o$ at the zero frequency limit are 3.99, The maximum static dielectric constant values are 5.75 at 4.50 eV. This energy corresponds to the ultraviolet region of the electromagnetic spectrum. The $KTaO_3:Cr^{3+},V_o$ has 4.30 at 1.65 eV, and this energy corresponds to the visible region of the electromagnetic spectrum. The formed peaks represent optical transitions of electrons passing from the valence band to the conduction band.

The absorption coefficient is a parameter, which determines the range of light that passes through the materials before being absorbed. The absorption spectra for undoped and doped compounds are shown in Fig .8. The peaks in different energies result from to electron transition from valence band to conduction band for both compounds $KTaO_3$ and $KTaO_3:Cr^{3+}$, V_o. The first peak for undoped $KTaO_3$ occurs at 6.10 eV, which correspond to the ultraviolet region in the electromagnetic spectrum. The first peak for $KTaO_3:Cr^{3+}$, V_o compound is beginning to form in the visible region. The absorption coefficients have reached the maximum value in the ultraviolet region for doped and undoped compound.

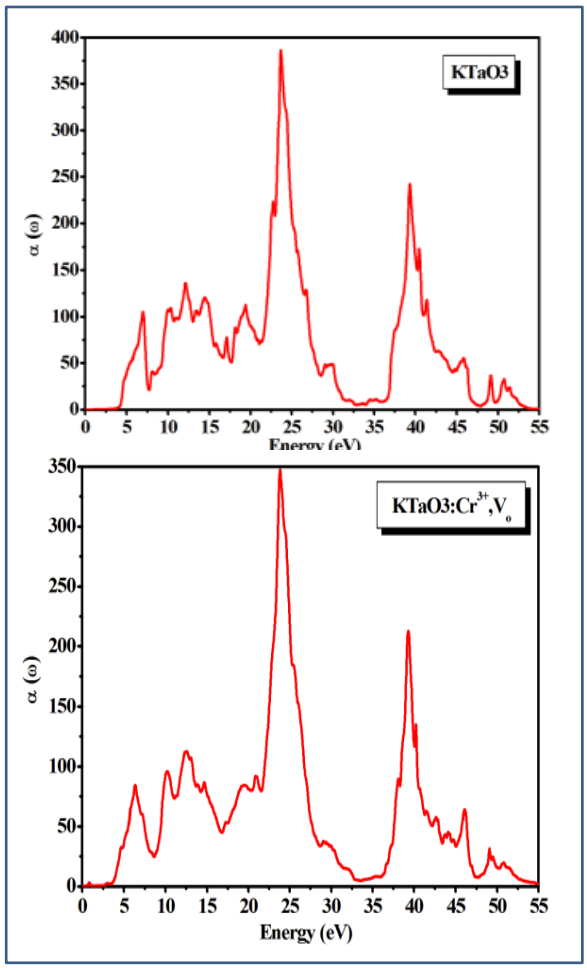

Figure 8. The calculated absorption spectra for $KTaO_3$ and KTaO3:Cr^{3+}, V_o

Refraction indices for undoped and doped compounds based on photon energy, are shown in Fig .9. The refractive index is the complex variable given as N(ω) = n(ω) + jk(ω), where k(ω) is called the extinction coefficient. The refraction index of undoped $KTaO_3$ compound is calculated at zero energy. The refraction indices for doped compound at the zero frequency limit is 2.14. As can be clearly seen the refraction indice increase with the effect of doping and defect.

The important optical constants like reflectivity R (ω), for both compounds are shown in Fig. 10. The calculated reflectivity at the zero energy limit for undoped and doped compounds have 0.1 and 0.15 respectively. As a result of this, the value reflection of doped compound has increased with the effect of doping and oxygen vacancy. In addition, an increase in reflectivity is a probable result. Because we know that the band gap energy is inversely proportional to reflectivity.

3.3 Magnetic properties of $KTaO_3$ and $KTaO_3$:Cr^{3+}, Vo

In the present work, we performed first principle calculations, using modified Becke Johnson potential mBJ-GGA, to study the magnetic properties of doped $KTaO_3$ with an oxygen vacancy.

To investigate and calculate the magnetic properties of the doped structure, we have optimized this compound ferromagnetically as well as antiferromagnetically. The stable state were found to be the ferromagnetic one with negative values of the total energy difference ΔE. The results of total, local and interstitial magnetic moments for $KTaO_3$:Cr^{+3}, V_o calculated using mBJ-GGA are given in table 3.

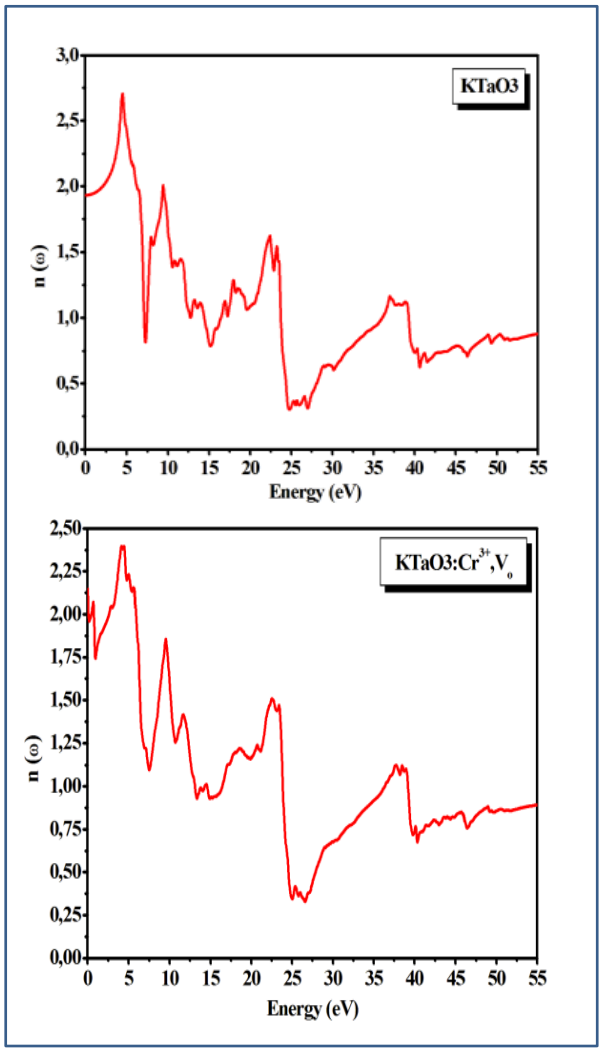

Figure 9. The calculated refraction index spectra for $KTaO_3$ and KTaO3:Cr^{3+}, V_o

Table 3: Total and partial magnetic moments (μ_B) for $KTaO_3$:Cr^{3+}, V_o

Compound	$KTaO_3$:Cr^{3+}, V_o
μ^T	2.97592
μ^K	0.00291
μ^{Ta}	0.15506
μ^{Cr}	2.11638
μ^I	0.70157

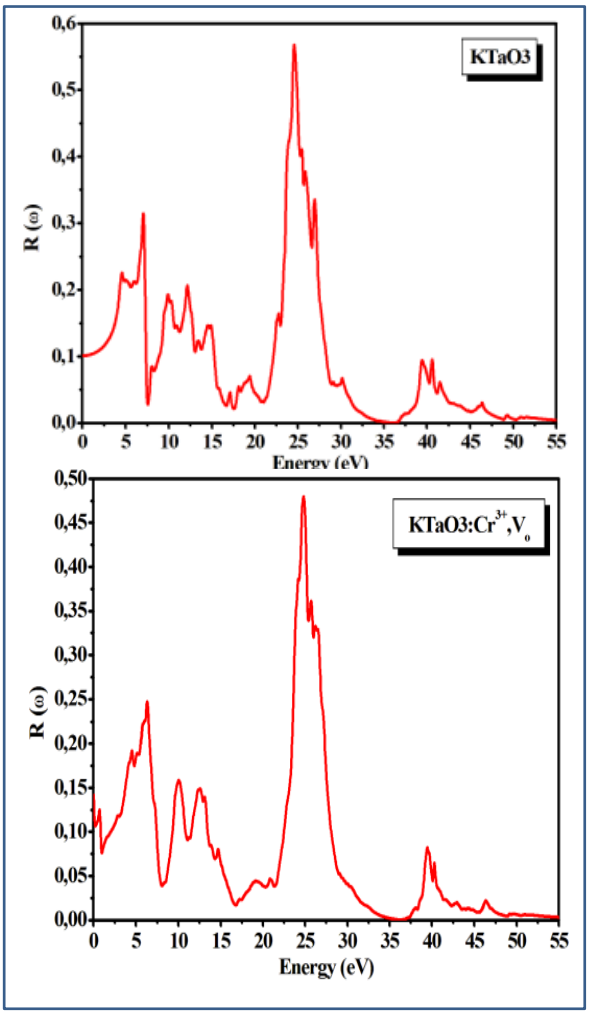

Figure 10. The calculated reflectivity spectra for $KTaO_3$ and $KTaO3:Cr^{3+}$, V_o

The positive values of the magnetic moments of the interstitial site and the other atoms : K, Ta and O confirm that they are alligned antiparallel to the magnetic moment of the chromium atom which is equal to 2.11638μ_B. We deduce from these results that the total magnetic moments which is equal to 2.97592 μ_B, comes essentially from the magnetic moment of Cr with a small contribution of oxygen site. The integer value of the total magnetic moment confirms that inserting a transition metal like chromium in this study affect considerably the structure and give us a new structure to get promising devices in spintronis.

4. Conclusion

In this work, we have investigated the electronic, optical and magnetic properties with the full potential linear augmented plane wave (FP-LAPW) method using general gradient approximation of undoped and Cr^{+3} doped defective $KTaO_3$ compounds.The defective structure has occured with the doping of Cr^{+3} atoms. To provide a charge balance, the oxygen vacancy is formed and causes a defect. The calculated structural parameters of cubic $KTaO_3$ are in good agreement with experimental values. TDOS and PDOS calculations have been performed to examine electronic properties for the two structures. For undoped compound the band gap energy is equal 3.59eV which is in a good agreement with literature. It has been found that for the KTaO3: Cr^{+3}, V_o; the band energy gap has decreased considerably. The results of optical properties indicate that the insertion of chromium and formation of defect can greatly improve the photocatalitics properties, which will further promote their applications in solid-state lighting. Beside, results for magnetic properties improve the utility of this structure in spin electronics field.

References

[1] D. Li, J. Zheng and Z. Zou, J. Phys. Chem. Solids, 67 (2006) 801.
[2] G. Pecchi, M. G. Jiliberto, A. Buljan and E. J. Delgado, Solid State Ionics, 187 (2011) 27.
[3] A. Jia, Z. Su, L. L. Lou and S. Liu, Solid State Sci, 12 (2010) 1140.
[4] B. Bajorowicz, A. Cybula, M. J. Winiarski, T. Klimczuk, A. Zaleska, Surface properties of Photocatalytic Activity of $KTaO_3$, CdS, MoS_2 Semiconductors and their Binary and Ternary Semiconductor Composites, Molecules. 19 (2014) 15339-15360.
[5] V. Vikhnin, S. Eden, M. Aulich, S. Kapphan, J. Solid State Communications. 113 (2000) 455.
[6] H. Kato, A. Kudo, J. Phys. Chem. B. 105 (2001) 4285.
[7] B. Modak, S.K. Ghosh, J. Solar Energy Materials & Solar Cells. 159 (2017) 590.
[8] E. Grabowska, J. Applied Catalysis B: Environmental, 186 (2016) 97.
[9] M. Petersen, F. Wagner, L. Hufnagel, M. Scheffler, P. Blaha, K. Schwarz, J. Computer Physics Communications, 126 (2000) 294.
[10] K. Schwarz, J. Solid State Chemistry. 176 (2003) 319.
[11] P. Blaha, K. Schwarz, G. K. H. Madsen, D. Kvsnicka, J. Luitz, Universitat, Wien, Austria, ISBN (2001) 3-9501031-1-2
[12] K. M. Wong, M. Irfan, A. Mahmood, and G. Murtaza, J. Optik 130 (2017) 517.
[13] K. M. Wong, S. M. Alay-e-Abbas, Y. Fang, A. Shaukat, and Y. Lei, J. Appl. Phys. 114 (2013) 034901.
[14] A. D. Becke, and E. R. Johnson, J. Chem. Phys. 124 (2006) 221101.
[15] F. Tran, and P. Blaha, Phys. Rev. Lett. 102 (2009) 226401.
[16] F. Birch, J. Phys. Rev, 71 (1947) 809.
[17] S. Cabuk, H. Akkus, A. M. Mamedov, J. Phys. B, 394 (2007) 81.
[18] S. Cabuk, J. Phys. Status Solidi B, 247 (2010) 93.
[19] R. Comes, G. Shirane, J. Phys. Rev. B 5 (1972) 1886.
[20] U. Hiromoto, T. Sakudo, J. Phys. Soc. Jpn. 38 (1975) 183.
[5] V. Vikhnin, S. Eden, M. Aulich, S. Kapphan, J. Solid State Communications. 113 (2000) 455.
[6] H. Kato, A. Kudo, J. Phys. Chem. B. 105 (2001) 4285.

[7] B. Modak, S.K. Ghosh, J. Solar Energy Materials & Solar Cells. 159 (2017) 590.
[8] E. Grabowska, J. Applied Catalysis B: Environmental, 186 (2016) 97.
[9] M. Petersen, F. Wagner, L. Hufnagel, M. Scheffler, P. Blaha, K. Schwarz, J. Computer Physics Communications, 126 (2000) 294.
[10] K. Schwarz, J. Solid State Chemistry. 176 (2003) 319.
[11] P. Blaha, K. Schwarz, G. K. H. Madsen, D. Kvsnicka, J. Luitz, Universitat, Wien, Austria, ISBN (2001) 3-9501031-1-2
[12] K. M. Wong, M. Irfan, A. Mahmood, and G. Murtaza, J. Optik 130 (2017) 517.
[13] K. M. Wong, S. M. Alay-e-Abbas, Y. Fang, A. Shaukat, and Y. Lei, J. Appl. Phys. 114 (2013) 034901.
[14] A. D. Becke, and E. R. Johnson, J. Chem. Phys. 124 (2006) 221101.
[15] F. Tran, and P. Blaha, Phys. Rev. Lett. 102 (2009) 226401.
[16] F. Birch, J. Phys. Rev, 71 (1947) 809.
[17] S. Cabuk, H. Akkus, A. M. Mamedov, J. Phys. B, 394 (2007) 81.
[18] S. Cabuk, J. Phys. Status Solidi B, 247 (2010) 93.
[19] R. Comes, G. Shirane, J. Phys. Rev. B 5 (1972) 1886.
[20] U. Hiromoto, T. Sakudo, J. Phys. Soc. Jpn. 38 (1975) 183.
[21] D. Li, J. Zheng and Z. Zou, J. Phys. Chem. Solids, 67 (2006) 801.
[22] G. Pecchi, M. G. Jiliberto, A. Buljan and E. J. Delgado, Solid State Ionics, 187 (2011) 27.
[23] A. Jia, Z. Su, L. L. Lou and S. Liu, Solid State Sci, 12 (2010) 1140.